Journal of the Meteorological Society of Japan, Vol. 90A, pp. 397–408, 2012.
DOI:10.2151/jmsj.2012-A24

NOTES AND CORRESPONDENCE

On the Mechanism of Tropical Cyclone Frequency Changes Due to Global Warming

Masato SUGI, Hiroyuki MURAKAMI

Japan Agency for Marine-Earth Science and Technology, Yokohama, Japan

and

Jun YOSHIMURA

Meteorological Research Institute, Tsukuba, Japan

(Manuscript received 9 May, in final form 29 October 2011)

Abstract

In order to explore the hypothesized mechanisms for the reduction of global tropical cyclone (TC) frequency due to greenhouse warming, an experiment has been conducted using a most recent version of MRI-AGCM with a new convection scheme. In addition to a present climate run (HPA run) and a future climate run (HFA run), two more runs are conducted. In CO2F run, future values of CO_2 and other greenhouse gas (GHG) concentrations are used with present value of sea surface temperature (SST), while in the SSTF run, future value of SST is used with present values of CO_2 and other GHG concentrations. The reductions of global TC frequency in HFA run, CO2F run and SSTF run from HPA run are 25%, 9% and 18%, respectively. These results are basically consistent with previous studies.

Based on the results of the experiment, we examined three key relations in our hypothesized mechanism for the reduction of TC frequency. First, the relation between changes in atmospheric radiative cooling and precipitation is confirmed to be valid in the experiment, in which not only CO_2 but other GHG is increased. It is also confirmed that the effect of increasing CO_2 is decreasing precipitation, while the effect of increasing other GHG is increasing precipitation. Second, the relation between changes in precipitation and upward mass flux is clarified by using a simple approximate thermodynamic equation. Third, regarding the relation between changes in upward mass flux and TC genesis frequency, we examined the changes in four parameters (precipitation, upward mass flux, vertical wind shear and mid-troposphere saturation deficit) which are closely related to deep convective activities in the tropics and may affect TC genesis frequency. The results of our experiment support the idea suggested by the previous studies that the reduction of TC frequency is closely related to a reduction of upward mass flux, although the chain of causality linking the two remains unclear. In addition, our experiment suggests a possibility that the changes in mid-troposphere saturation deficit may also contribute to the changes in TC genesis frequency.

1. Introduction

Recent high resolution (grid size of about 100 km or finer) model experiments consistently show that the global tropical cyclone (TC) frequency is likely to decrease in the future greenhouse gas warmed climate, while number of very intense TCs may increase (Kunutson et al. 2010). The reduction of global TC frequency due to global warming was first shown by Bengtsson et al. (1996). They suggested that the reduction of TC frequency might be related to the changes in Hadley circulation and subtropical jets. Sugi et al.

Corresponding author: Masato Sugi, Japan Agency for Marine-Earth Science and Technology, 3173-25 Showa-machi, Kanazawa-ku, Yokohama, Kanagawa, 236-0001, Japan.
E-mail: msugi@jamstec.go.jp

(2002) also showed the reduction of global TC frequency due to global warming and suggested that the reduction of TC frequency is closely related to the weakening of tropical circulation (reduction of upward mass flux). It has been shown that the weakening of tropical circulation or reduction of upward mass flux is a robust feature of the climate change associated with the GHG increase (Held and Soden 2006; Vecchi and Soden 2007). On the other hand, Emanuel et al. (2008) proposed a different mechanism for the reduction of global TC frequency based on their downscaling experiment. They suggested that the reduction of the TC frequency is closely associated with the increase in mid-troposphere saturation deficit due to global warming.

To explore the mechanism of the reduction of global TC frequency, Yoshimura and Sugi (2005) (YS05 hereafter) conducted an experiment to examine the effect of CO_2 increase and SST increase separately. They concluded that TC frequency is significantly reduced when CO_2 is increased with fixed SST, while TC frequency changes little when SST is increased with fixed CO_2. Based on the experiment, they suggested a following mechanism (hypothesis) for the reduction of TC frequency due to global warming. When only CO_2 is increased, precipitation is significantly reduced (Sugi and Yoshimura 2004) and associated upward mass flux is reduced, with a significant reduction of TC frequency. On the other hand, when only SST is increased, precipitation significantly increased, but due to a significant increase of static stability, upward mass flux changes little, with little change in TC frequency. Recently, Held and Zhao (2011) conducted a similar experiment as YS05 and have shown that the effects on the reduction of TC frequency of doubling CO_2 and increasing SST by 2K are about the same. We believe that YS05 is a useful experiment to explore the mechanism of the reduction of TC frequency, but until recently YS05 was the only one experiment which examined CO_2 effect and SST effect separately on the TC frequency change. We recently conducted an experiment similar to YS05 using a most recent version of the MRI-AGCM. This is basically a follow-up experiment of YS05, and main objective of the experiment is to further explore the mechanism suggested by previous studies of the reduction of TC frequency due to global warming. However, the experiment is conducted with a little more realistic setting to examine the mechanism of TC frequency reduction in a realistic future projection experiment. It also should be noted that the physics schemes in the new MRI-AGCM, particularly the deep cumulus convection scheme and radiation scheme, are very different from those used in YS05.

2. Model and experiments

The model we used for the experiment is a most recent version of the Meteorological Research Institute (MRI) Atmospheric General Circulation Model, MRI-AGCM3.2 (Mizuta et al. 2012). In the new model, a cumulus convection scheme developed by H. Yoshimura is employed (Yukimoto et al. 2012), which has significantly improved tropical precipitation climatology and TC simulations (Mizuta et al. 2011). Four 25-year simulations have been conducted using the 60 km resolution version of the MRI-AGCM3.2 with prescribed sea surface temperature (SST) and greenhouse gas (GHG) including CO_2 and aerosols (Table 1). For the present climate simulation (HPA run, present climate run), the observed SST for the 25 year period from January 1979 to December 2003 (HadISST1, Rayner et al. 2003) and observed GHG concentration are prescribed. For the standard future climate simulation (HFA run), the average SST increase for the 25 year period from January 2075 to December 2099 projected by CMIP3 models is added to the SST used for the HPA run. For the HFA run, GHG concentration including CO_2

Table 1. Experiments.

Name (Short Name)	Experiment (Run)	SST	GHG
HPA (P)	Present day climate simulation 1979–2003	Present	Present
HFA (F)	Future climate simulation 2075–2099	Future	Future
CO2F (CF)	Future CO2 simulation 2075–2099	Present	Future
SSTF (SF)	Future SST simulation 2075–2099	Future	Present

and aerosols for the same period based on A1B scenario is prescribed. Two additional runs are conducted to study the effect of GHG change and SST change separately on the TC frequency. In the future CO_2 (CO2F) run, GHG including CO_2 and aerosols for the HFA run and SST for HPA run are used, while in the future SST (SSTF) run, GHG including CO_2 and aerosols for the HPA run and SST for the HFA run are used. The detection algorithm of TC genesis in the simulations is the same as that used in Murakami and Sugi (2010). It should be noted that the experiment of YS05 is an idealized experiment, in which only CO_2 is considered as GHG, aerosols are not included and SST is uniformly changed. On the other hand, the experiment of the present study is conducted under a little more realistic setting as described above.

3. Global TC frequency change

Figure 1a shows the changes in global or hemispheric TC frequency of SSTF, CO2F and HFA runs from HPA run. The global TC frequency of HFA run is less than that of HPA run by about 25%, while the TC frequencies of SSTF run and CO2F run are less than those of HPA run by about 9 and 18%, respectively. As indicated by error bars in Fig. 1(a), there is a large uncertainty in the rate of reduction of TC frequency in the experiment. However, the difference between the rates of reduction for CO2F run and SSTF run is statistically significant at 90% significance level. Figure 1b shows the changes in upward mass flux (upward *p*-velocity) at 500 hPa level averaged over the ocean region from 5°N to 30°N for the Northern Hemisphere and from 5°S to 30°S for the Southern Hemisphere. The average is taken over the grid points where the monthly mean vertical velocity is upward. The average is also taken over the TC season of each hemisphere (six months from June to November for Northern Hemisphere and four months from January to April for Southern Hemisphere). The rate of reduction in upward mass flux is about 6% for HFA run, 2% for CO2F run and 2.4% for SSTF run. There is a large uncertainty in the rate of reduction of upward mass flux as well, as indicated by the error bars in Fig. 1(b).

A recent study by Held and Zhao (2011) showed about 10% reduction of global TC frequency for both doubling CO_2 and 2K increase in SST. YS05 also showed 13% and 12% reduction of global TC frequency for doubling CO_2 and 2K increase in SST, respectively, although they concluded that the effect of CO_2 increase is much larger than that of SST increase based on their results from quadrupling CO_2 and 2K decreasing SST experiments. These studies suggest that the effects on TC frequency reduction of CO_2 increase and SST increase are roughly the same. On the other hand, Fig. 1(a) indicates that the rate of reduction in TC frequency in CO2F run is smaller than that of SSTF run. One possible reason for this difference is the difference in experiment setting. The CO2F experiment of the present study includes the changes not only in CO_2 but also in other GHG and aerosols that may make

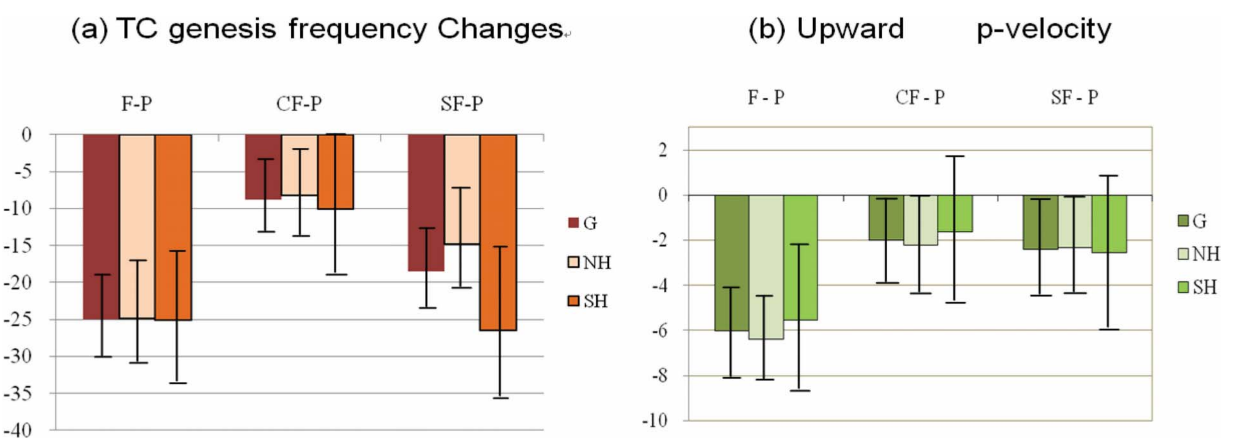

Fig. 1. (a) TC frequency changes of HF (F), CO2F (CF) and SSTF (SF) runs from HPA (P) run. Unit is %. (b) Same as (a) but for upward mass flux (*p*-velocity) at 500 hPa averaged over the tropical ocean (5°N–30°N, 5°S–30°S) and respective TC season (NH: JUN–NOV, SH: JAN–APR). Error bars indicate the 90% confidence interval estimated by *t*-test.

the effect of CO2 increase reduced (see next section for more discussion). Another possibility is that the difference between the rates of reduction of TC frequency for CO2F run and SSTF run is not real, even though it is statistically significant. We have noted that the difference between the CO2F run and SSTF run is not statistically significant when TC frequency is computed by using somewhat different detection criteria as used in Oouchi et al. (2006). Considering this and the large uncertainty indicated by the error bars in Fig. 1, a further detailed quantitative discussion would be difficult at this stage.

4. Mechanism of the reduction of global TC frequency

A whole picture of the mechanism (hypothesis) of the reduction of global TC frequency due to global warming suggested by previous studies (Sugi et al. 2002; Sugi and Yoshimura 2004, YS05) is illustrated in Fig. 2. It should be noted that the boxes and arrows in Fig. 2 do not represent time sequences but logical sequences. The arrows in Fig. 2 represent that the changes in the left hand side boxes are the reason for the changes in the right hand side boxes, while the double lines indicate that the changes in the left hand side boxes are simultaneously occurring with the changes in the right hand side boxes. There are three key relations involved in the suggested mechanism: relations between 1) radiative cooling and precipitation, 2) precipitation and upward mass flux, and 3) upward mass flux and TC genesis frequency. We examine in the following whether results of the present study are consistent with these three relations.

We first examine the relation between the changes in atmospheric radiative cooling and precipitation. Table 2a and b show the energy components of the global atmosphere and tropical atmosphere, respectively. The first row of each table shows the atmospheric energy components for present climate run (HPA run). In the global atmosphere, precipitation (condensation heating) and sensible heating from the surface are balanced by net radiative cooling. On the other hand, in the tropics, precipitation is almost balanced by net radiative cooling, and sensible heating from the surface is almost the same as residual which is transported to higher latitudes. The second, third and forth rows of each table show the changes in energy component of HFA, CO2F and SSTF runs from HPA run. The change in precipitation is negative for CO2F run, while it is positive for SSTF run. These changes correspond well to the changes in net radiative cooling, and consistent with the relations shown in Fig. 2. Note that the reduction of tropical mean precipitation in the CO2F run is 2.3% (2.3 Wm^{-2}/101.2 Wm^{-2}), which is less than that of 3% in the doubling CO_2 experiment of YS05. This difference is expected, because the pres-

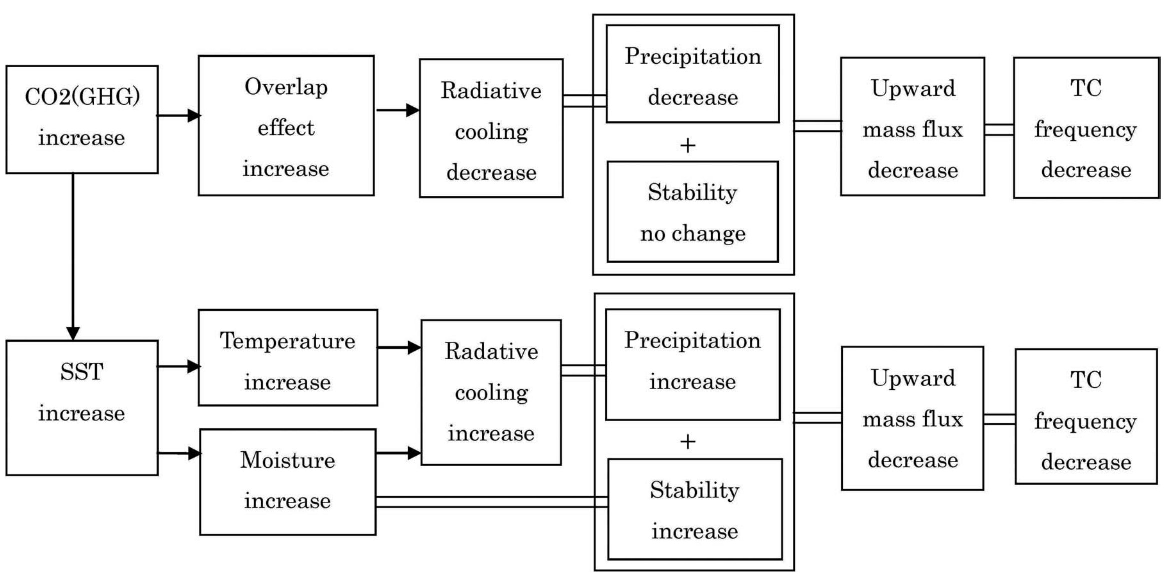

Fig. 2. Schematic diagram of the proposed mechanism of TC frequency reduction.

Table 2. Area averaged annual mean atmospheric energy components of HPA run (first row) and their changes in HFA, CO2F and SSTF runs from HPA run (second to fourth rows) for (a) global atmosphere and (b) tropical atmosphere (30°N–30°S). Unit is W m^{-2}. CS indicates clear sky.

(a) Global Atmosphere							
	Precipitation	LW Cooling	SW Heating	Rad Cooling	CS Rad Cooling	Sensible Heating	Residual
P	85.3	178.7	76.2	102.5	109.8	16.9	−0.2
F–P	4.8	6.4	2.4	4.0	5.0	−0.7	0.1
CF–P	−1.7	−1.4	0.6	−2.0	−2.1	−0.3	0.0
SF–P	6.8	8.1	1.6	6.5	7.6	−0.2	0.0
(b) Tropical Atmosphere							
	Precipitation	LW Cooling	SW Heating	Rad Cooling	CS Rad Cooling	Sensible Heating	Residual
P	101.2	195.3	90.9	104.4	123.2	21.8	18.6
F–P	4.8	7.5	2.8	4.7	5.6	−0.4	−0.2
CF–P	−2.3	−1.8	0.5	−2.3	−2.6	−0.4	−0.4
SF–P	7.3	9.6	1.9	7.7	9.0	0.2	−0.2

ent experiment setting is a little different from that of YS05. In the CO2F run, not only CO_2 but other GHG and aerosols are changed. In doubling CO_2 experiment of YS05, most of the change in radiative cooling is the reduction of long wave cooling due to overlap effect of CO_2 and water vapor long wave absorption bands (Sugi and Yoshimura 2004). The reduction of long wave cooling in this experiment can be estimated to be 3 Wm^{-2}. The reduction of long wave cooling due to CO_2 increase in the CO2F run should be almost the same as this. Therefore, the effect of the other GHG is estimated to be increasing long wave cooling by 1.2 Wm^{-2}. Moreover, Table 2 shows that the changes in shortwave heating significantly contribute to the changes in net radiative cooling, even in the CO2F run. The short wave heating increase in CO2F run is probably due to black carbon aerosol. Table 2 also shows that the effects of clouds, indicated by the difference between the net radiative cooling and clear sky (CS) radiative cooling, are not negligible and can affect the changes in net radiative cooling and precipitation. It should be noted that the energy balance of global or tropical atmosphere constrain only the global mean or tropical mean precipitation. The changes in regional precipitation can be different from the changes in global or tropical mean precipitation.

Next, we examine the relation between the changes in precipitation and upward mass flux. Table 3 shows the fractional changes in precipitation P, upward mass flux (p-velocity) at 500 hPa ω and dry static stability S (defined as difference between potential temperature at 200 hPa and 850 hpa) for HPA, CO2F and SSTF runs. P, ω and S are averaged over the tropical oceans (5°N–30°N and 5°S–30°S) and respective TC seasons (NH: Jun–Nov, SH: Jan–Apr). The fractional changes in precipitation shown in the first column of Table 3 are a little

Table 3. Fractional changes in precipitation (P), upward mass flux at 500 hPa (ω), their difference and dry static stability at 500 hPa (S) averaged over the tropical ocean (5°N–30°N, 5°S–30°S) and respective TC season (NH: JUN–NOV, SH: JAN–APR). Unit is %.

		$\frac{\Delta P}{P}$	$\frac{\Delta\omega}{\omega}$	$\frac{\Delta P}{P}-\frac{\Delta\omega}{\omega}$	$\frac{\Delta S}{S}$
NH	F–P	5.8	−6.4	12.2	12.1
	CF–P	−3.8	−2.2	−1.6	0.0
	SF–P	10.5	−2.3	12.8	12.2
SH	F–P	5	−5.5	10.5	11.2
	CF–P	−4.4	−1.6	−2.8	0.0
	SF–P	9	−2.5	11.5	11.0

larger than the fractional changes in precipitation calculated from the energy changes in the first column of Table 2. This indicates that the changes in precipitation over the ocean are larger than the tropical average. Table 3 indicates that both the precipitation and upward mass flux decrease in CO2F run. On the other hand, in HFA run and SSTF run, precipitation increases but upward mass flux decreases. How can we understand these relations between the precipitation and upward mass flux changes? Over the precipitating area in the tropics, an approximate form of thermodynamic equation can be written as

$$\omega S \approx \alpha P, \tag{1}$$

where α is a scaling constant (Holton 1979). If the temporal and spatial variation of S is small, compared with the variation of ω and P, then the equation also holds for area mean or time mean of ω and P. From Eq. (1), we can derive a following relation for fractional changes of P, ω and S.

$$\frac{\Delta\omega}{\omega} \approx \frac{\Delta P}{P} - \frac{\Delta S}{S}. \tag{2}$$

Comparison of the third and fourth column of Table 3 indicates that Eq. (2) is a good approximation for P, ω and S averaged over the tropical oceans and TC season of respective hemisphere. Thus, we can understand the relation between the changes in precipitation and upward mass flux by Eq. (2), in which the change of stability is playing an important role.

Finally, we examine the relation between the changes in upward mass flux and TC genesis frequency. This relation may be most important but most uncertain—and least understood—link in the whole proposed mechanism shown in Fig. 2. Previous studies suggested that the reduction of TC frequency is closely related to a decrease of upward mass flux. Present study also shows the reduction of global TC frequency and reduction of upward mass flux (Fig. 1). We have noted, however, there are large uncertainties both in the changes in TC frequency and upward mass flux. Moreover, it has not been well understood how the reduction of upward mass flux is related to the reduction of TC frequency. TC genesis is closely related to activities of deep cumulus convections. For a TC scale vortex development, low-level mass convergence associated with ensemble of deep cumulus convections is needed. We speculate that this requirement leads to a close relationship between TC genesis frequency changes and the changes in intensity of the long-term mean upward mass flux in our model, although the details of this relationship remain unclear. In the next section, we examine the changes in convective activity and their relation with TC frequency change.

5. Changes in deep convective activities

We can expect that the TC genesis and its changes are related in some way to the overall activity of deep convection in the tropics. Here, we examine four parameters which are closely related to deep convective activity in the tropics: precipitation, upward mass flux, vertical wind shear and mid-troposphere saturation deficit. Figure 3a shows the TC genesis counts in 5° latitude by 5° longitude grid boxes in the 25 year simulation of HPA run (present climate run). Figure 3b shows the geographical distribution of precipitation in HPA run averaged over the TC season of each hemisphere (6 months from June to November in Northern Hemisphere and 4 months from January to April in Southern Hemisphere). Comparison of Fig. 3a with Fig. 3b shows that the most TC genesis occurs within the active convection area indicated by the seasonal mean precipitation exceeding 4 mm/day. Figure 3c shows the geographical distribution of upward mass flux at 500 hPa in HPA run averaged over the TC season of each hemisphere. The mean upward mass flux is calculated at each grid point by using only negative monthly mean p-velocity data. The area of upward mass flux also represents the area of active deep convection and almost identical with the area of intense precipitation shown in Fig. 3b. In addition to precipitation and upward mass flux, we consider here two more parameters: vertical wind shear and saturation deficit, which are closely related to tropical deep convective activities and have been considered to be important environmental parameters for TC genesis (Gray 1975, Emanuel and Nolan 2004, Emanuel et al. 2008). Figure 3d shows the geographical distribution of vertical wind shear (magnitude of the difference in vector winds at 200 hPa and 850 hPa) in HPA run averaged over the TC season of each hemisphere. We can see that the geographical distribution of the vertical wind shear roughly agree with that of convective activity indicated by precipitation in Fig. 3b. The vertical wind shear tends to be small over the active convection centers. Figure 3e shows the geographical distribution of saturation deficit

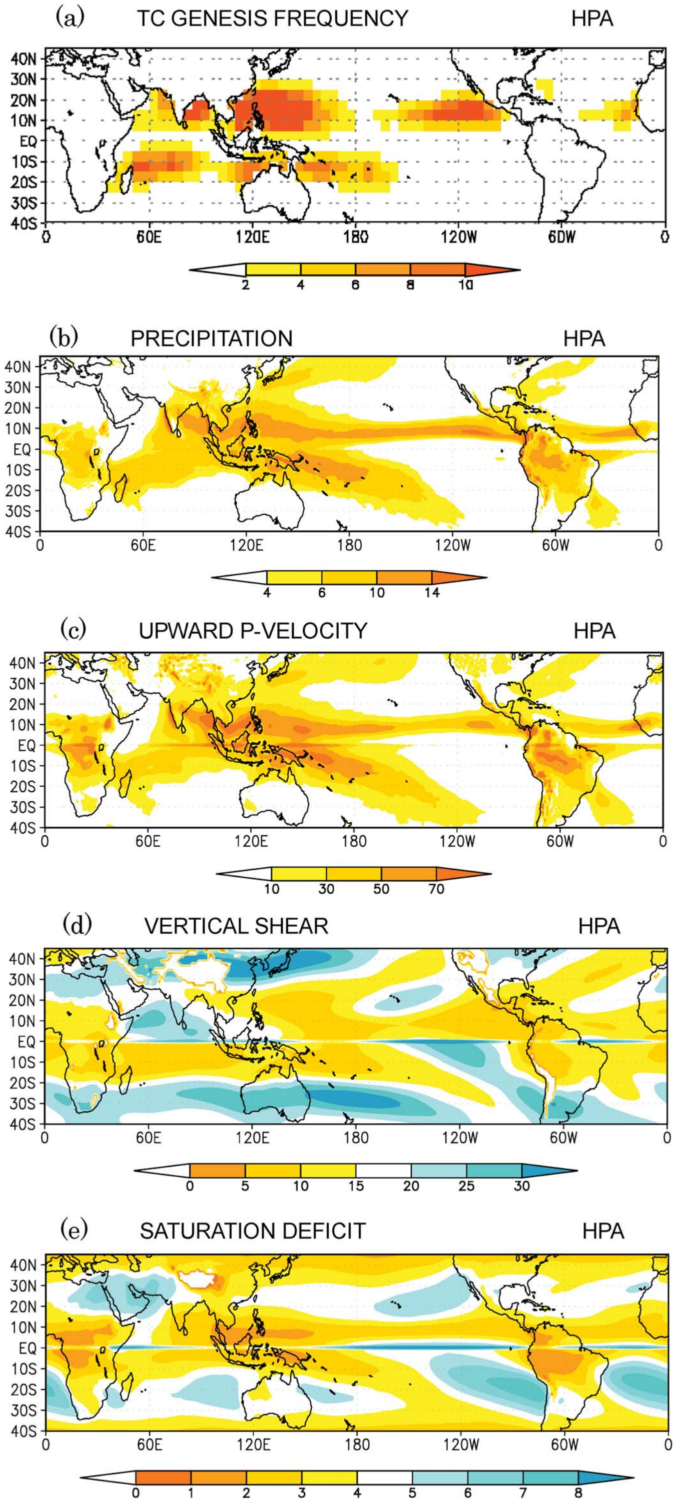

Fig. 3. (a) TC genesis frequency (number in $5° \times 5°$ grid box per 25 year), (b) Precipitation (mm/day), (c) Upward mass flux (hPa/hour), (d) Vertical wind shear between 200 hPa and 850 hPa (m/s), and (e) Saturation deficit at 600 hPa (g/kg) in HPA run (present climate run). In (b)–(e), each variable is averaged over TC season of respective hemisphere (NH: JUN–NOV, SH: JAN–APR).

at 600 hPa in HPA run averaged over the TC season of each hemisphere. We can see that the geographical distribution of the saturation deficit also roughly agree with that of convective activity indicated by precipitation in Fig. 3b. The saturation deficit tends to be small over the active convection areas.

Figure 4 shows the geographical distribution of the changes between CO2F run and HPA run in TC genesis frequency and the four parameters: precipitation, upward mass flux, vertical wind shear and mid-troposphere saturation deficit. In CO2F run, the distributions of the changes in precipitation and upward mass flux (Fig. 4b and 4c) agree very well with each other, and they agree with the distribution of the changes in TC genesis frequency (Fig. 4a) as well. Note that the agreement of the distribution of the changes in precipitation and upward mass flux is expected from Eq. (2), as the stability does not change in CO2F run and the second term of Eq. (2) is negligible. On the other hand, the changes in the vertical wind shear and saturation deficit in CO2F run (Fig. 4d and 4e) appear to be too small to produce the significant reduction of TC genesis frequency.

Figure 5 shows the geographical distribution of the changes in TC genesis and four parameters between SSTF run and HPA run. In SSTF run, precipitation increases almost everywhere (Fig. 5b), while upward mass flux increases over the region where the precipitation increases significantly but decreases in other regions. It should be noted, however, that the changes in precipitation and upward mass flux is consistent with Eq. (2) in the SSTF run as well. Indeed, the distribution of upward mass flux change shown in Fig. 6, which is computed by using Eq. (2) from the precipitation change in Fig. 5b with the precipitation and upward mass flux of HPA run (Fig. 3b and c), agrees well with the upward mass flux change shown in Fig. 5c, although the amplitude is a little smaller in Fig. 6. Unlike the CO2F run, the distribution of the upward mass flux change in SSTF run (Fig. 5c) does not agree well with the distribution of TC frequency change (Fig. 5a), except for the western North and South Pacific. This disagreement may be explained to some extent by the changes in vertical wind shear and saturation deficit in SSTF run, which are large compared with those of CO2F run and might be able to produce a significant change in TC genesis frequency. A relatively large increase in vertical wind shear over the eastern Pacific and North Atlantic may contribute to the reduction of TC genesis frequency there. On the other hand, an overall increase in the saturation deficit in SSTF run may contribute to the larger decrease of global TC frequency in SSTF run than in CO2F run as shown in Fig. 1a.

6. Summary and discussion

In order to examine the robustness of the possible mechanism for the reduction of global TC frequency due to greenhouse warming suggested by previous studies (Sugi et al. 2002; Sugi and Yoshimura 2004, YS05), an experiment similar to YS05 has been conducted using a most recent version of MRI-AGCM. In addition to a present climate run (HPA run) and a future climate run (HFA run), two more runs are conducted. In CO2F run, future values of CO_2 and other greenhouse gas (GHG) concentrations are used with present value of sea surface temperature (SST), while in the SSTF run, future value of SST is used with present values of CO_2 and other GHG concentrations. The reductions of global TC frequency in HFA run, CO2F run and SSTF run from HPA run are 25%, 9% and 18%, respectively. These results are basically consistent with previous studies.

Based on the results of the experiment, we examined three key relations in the mechanism of the reduction of TC frequency suggested by previous studies. First, the relation between the changes in atmospheric radiative cooling and precipitation is confirmed in our experiments, in which not only CO_2 but other GHG is increased. It is also confirmed that the effect of increasing CO_2 is decreasing long wave cooling and precipitation, while the effect of increasing other GHG is increasing long wave cooling and precipitation. Second, the relation between changes in precipitation and upward mass flux is clarified by using a simple approximate thermodynamic equation. The relation is found to be valid not only global scale but also on local scale. Third, regarding the relation between changes in upward mass flux and TC genesis frequency, we examined the changes in four parameters (precipitation, upward mass flux, vertical wind shear and mid-troposphere saturation deficit) which are closely related to deep convective activities in the tropics and may affect TC genesis frequency. We have noted that the tropical precipitation decreases in the CO2F run, while it increases in the SSTF run. Despite the opposite sign of the changes in precipitation, both runs show a significant decrease in

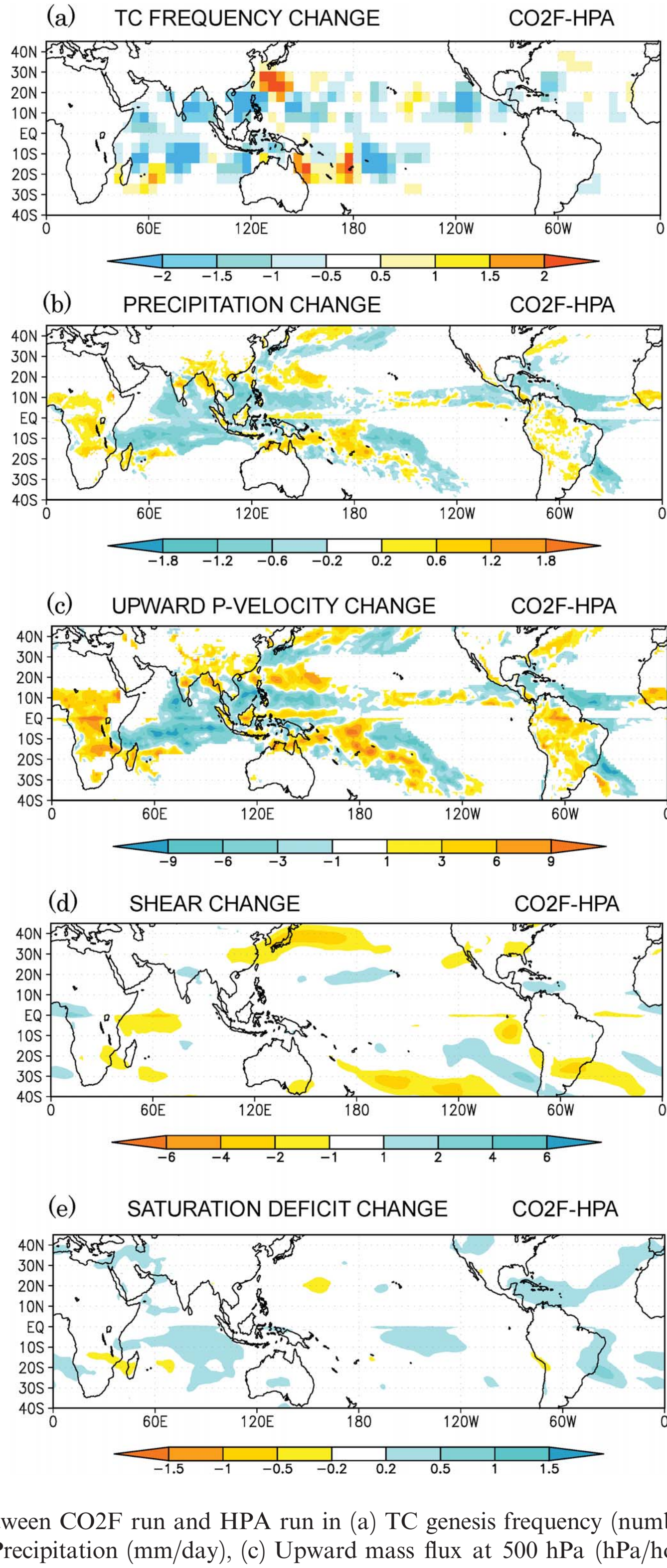

Fig. 4. Changes between CO2F run and HPA run in (a) TC genesis frequency (number in $5^\circ \times 5^\circ$ grid box per 25 year), (b) Precipitation (mm/day), (c) Upward mass flux at 500 hPa (hPa/hour), (d) Vertical wind shear between 200 hPa and 850 hPa (m/s), and (e) Saturation deficit at 600 hPa (g/kg). Each variable is averaged over TC season of respective hemisphere (NH: JUN–NOV, SH: JAN–APR).

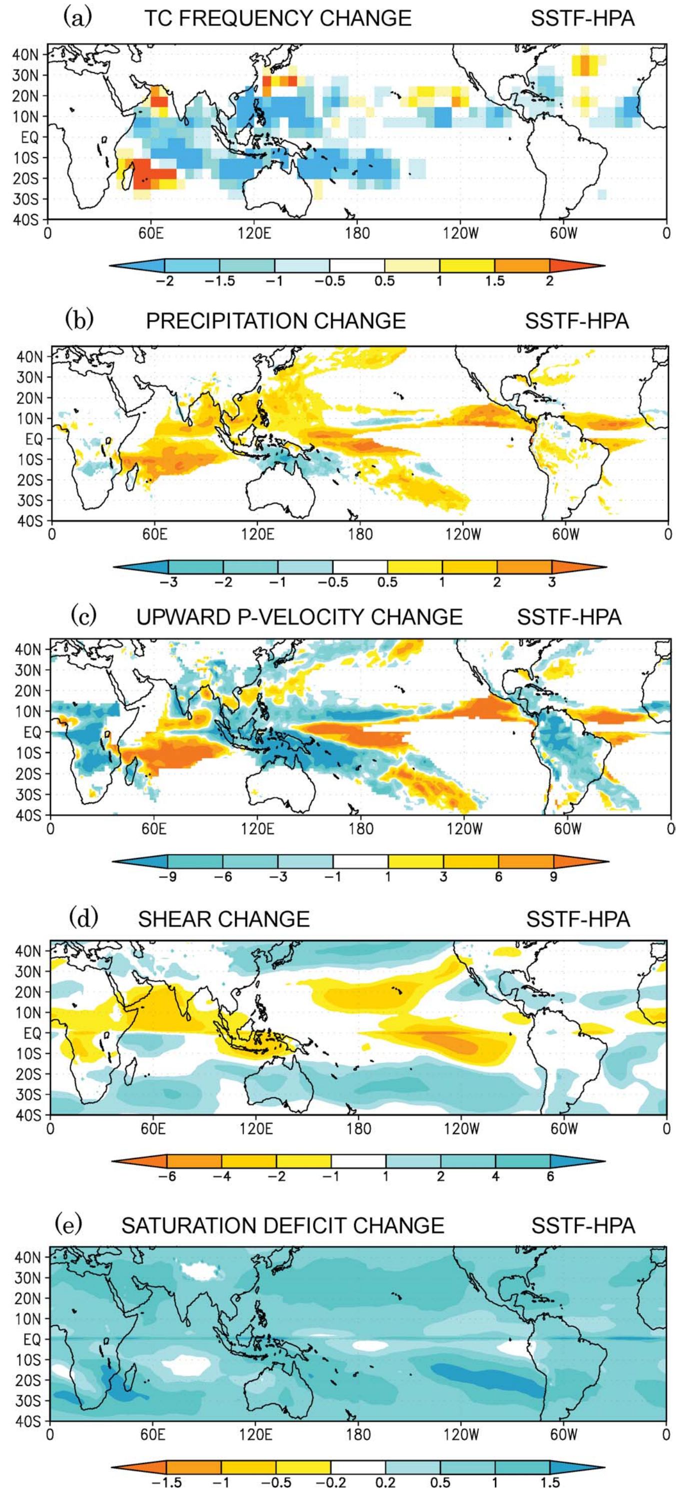

Fig. 5. Same as Fig. 4 but for the changes between SSTF run and HPA run.

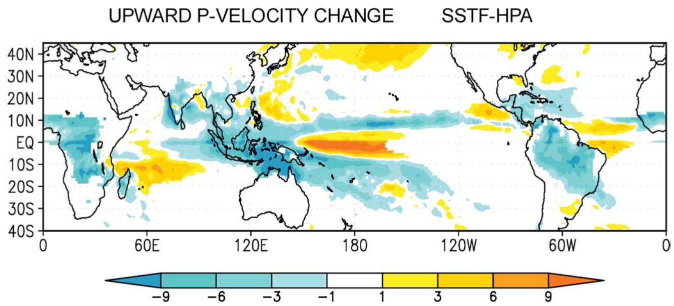

Fig. 6. Change in upward p-velocity between SSTF run and HPA run computed from precipitation change and using the equation (2).

upward mass flux and reduction in TC frequency. These results support the idea suggested by the previous studies that the reduction of TC frequency related to a reduction of upward mass flux, although the precise mechanism of the relationship between the two—and whether it is causal—remains unclear. We have also noted that the changes in saturation deficit are very little in the CO2F run despite a significant TC frequency reduction, while they are large in the SSTF run and may significantly contribute to the changes in TC genesis frequency.

One important remaining question is how a few percent reduction of seasonal mean mass flux causes a significant reduction of TC genesis frequencies. Held and Zhao (2011) argue that decreased mass flux makes it easier for advection of dry air to suppress genesis. We speculate that the reduction of upward mass flux is closely related to a weakening of TC scale low-level mass convergence associated with ensemble of deep cumulus convections, which is needed for a TC scale vortex development. A reduction of upward mass flux could make a weakening of low-level mass convergence and a reduction of TC-scale vortex development. However, since TC genesis occurs in a few days to a week time scale, we need to examine the changes in upward mass flux on this time scale in the experiment by using daily data. This should be an important subject of our future work: to understand how the reduction of seasonal mean upward mass flux can affect TC genesis in the model, and ultimately to explore for this relationship in the real world.

Acknowledgements

This work was conducted under the framework of the ‘‘Projection of the Change in future Weather Extremes using Super-high-resolution Atmospheric Models’’ supported by the KAKUSHIN Program of the Ministry of Education, Culture, Sports, Science, and Technology (MEXT). The calculations were performed on the Earth Simulator.

References

Bengtsson, L., M. Botzet, and M. Esch, 1996: Will greenhouse gas-induced warming over the next 50 years lead to higher frequency and greater intensity of hurricanes? *Tellus*, **48A**, 57–73.

Emanuel, K., R. Sundararajan, and J. Williams, 2008: Hurricanes and global warming: results from downscaling IPCC AR4 simulations. *Bull. Amer. Meteor. Soc.*, **89**, 347–367.

Emanuel, K., and D. Nolan, 2004: Tropical cyclones and the global climate system. Preprints, *26th AMS Conference on Hurricanes and Tropical Meteorology, Miami, FL.*

Gray, W. M., 1975: Tropical cyclone genesis. Dept. of Atmos. Sci. Paper No. 234, Colorado State University, Fort Collins, CO, 121 pp.

Held, I. M., and B. J. Soden, 2006: Robust responses of the hydrological cycle to global warming. *J. Climate*, **19**, 5686–5699.

Held, I. M., and M. Zhao, 2011: The response of tropical cyclone statistics to an increase in CO_2 with fixed sea surface temperatures. *J. Climate*, in press.

Holton, J., 1979: *An Introduction to Dynamic Meteorology*, Academic Press, 391 pp.

Knutson, T., J. McBride, J. Chan, K. Emanuel, G. Holland, C. Landsea, I. Held, J. P. Kossin, A. Srivastava, and M. Sugi, 2010: Tropical cyclones and climate change. *Nature Geoscience*, p. doi:10.1038/ngeo0779.

Mizuta, R., H. Yoshimura, H. Murakami, M. Matsueda, H. Endo, T. Ose, K. Kamiguchi, M. Hosaka, M. Sugi, S. Yukimoto, S. Kusunoki, and A. Kitoh, 2012: Climate simulations using MRI-AGCM with 20-km grid. *J. Meteor. Soc. Japan*, **90A**, 233–258.

Murakami, H., and M. Sugi, 2010: Effect of model resolution on tropical cyclone climate projections. *SOLA*, **6**, 73–76, doi:10.2151/sola.2010-019.

Oouchi, K., J. Yoshimura, H. Yoshimura, R. Mizuta, S. Kusunoki, and A. Noda, 2006: Tropical cyclone climatology in a global-warming climate as simulated in a 20 km-mesh global atmospheric model: Frequency and wind intensity analysis. *J. Meteor. Soc. Japan*, **84**, 259–276.

Rayner, N. A., D. E. Parker, E. B. Horton, C. K. Folland, L. V. Alexander, and D. P. Rowell, 2003: Global analysis of sea surface temperature, sea ice, and night marine air temperature since the late nineteenth century. *J. Geophys. Res.*, **108**, 4407.

Sugi, M., A. Noda, and N. Sato, 2002: Influence of the global warming on tropical cyclone climatology: An experiment with the JMA Global Model. *J. Meteor. Soc. Japan*, **80**, 249–272.

Sugi, M., and J. Yoshimura, 2004: A mechanism of tropical precipitation change due to CO_2 increase. *J. Climate*, **17**, 238–243.

Vecchi, G. A., and B. J. Soden, 2007: Global warming and the weakening of the tropical circulation. *J. Climate*, **20**(17), 4316–4340.

Yoshimura, J., and M. Sugi, 2005: Tropical cyclone climatology in a high-resolution AGCM—Impacts of SST warming and CO_2 increase. *SOLA*, **1**, 133–136, doi:10.2151/soda.2005-035.

Yukimoto, S., H. Yoshimura, M. Hosaka, T. Sakami, H. Tsujino, M. Hirabara, T. Y. Tanaka, M. Deushi, A. Obata, H. Nakano, Y. Adachi, E. Shindo, S. Yabu, T. Ose, and A. Kitoh, 2011: Meteorological Research Institute-Earth System Model v1 (MRI-ESM1)—Model description—. *Tech. Rep. Meteor. Res. Inst.*, No. 64, 83 pp.